Q. J. R. Meteorol. Soc. (2003), **129**, pp. 3265–3275 doi: 10.1256/qj.02.211

Summertime low-ozone episodes at northern high latitudes

By Y. J. ORSOLINI[1]*, H. ESKES[2], G. HANSEN[1], U.-P. HOPPE[3], A. KYLLING[1], E. KYRÖ[4], J. NOTHOLT[5], R. VAN DER A[2] and P. VON DER GATHEN[6]

[1]*Norwegian Institute for Air Research, Kjeller, Norway*
[2]*Royal Netherlands Meteorological Institute, De Bilt, the Netherlands*
[3]*Norwegian Defence Research Establishment, Kjeller, Norway*
[4]*Finnish Meteorological Institute, Sodankyla, Finland*
[5]*University of Bremen, Germany*
[6]*Alfred-Wegener Institute for Polar and Marine Research, Potsdam, Germany*

(Received 11 November 2002; revised 7 April 2003)

SUMMARY

A pool of low-ozone air resides in the Arctic stratosphere in summer. Its formation and maintenance arise from a combination of chemical ozone-destruction and transport processes. The summertime ozone destruction is induced by gas-phase chemistry dominated by nitrogen and hydrogen catalytic cycles, which are efficient due to long summertime insolation at high latitudes. It is shown that, during events referred to as low-ozone episodes (LOEs), column ozone can locally decrease to values comparable with the seasonal minimum. A combination is used of (i) assimilation of satellite ozone observations from the Global Ozone Monitoring Experiment, (ii) chemical trajectory modelling, and (iii) the gathering of new lidar and *in situ* ozone observations in the European Arctic in summer 2000. Hence it is shown that such LOEs involve the displacement of the pool of low-ozone air in the middle stratosphere, which is more dynamic than previously thought and undergoes pronounced meridional excursions, in particular towards northern Europe. The thinner the ozone layer, the more ultraviolet (UV) radiation reaches the ground, where it can impact on human health and ecosystems. Erythemal UV dose enhancements of the order of 10–15% were observed in northern Norway during the LOEs in summer 2000.

KEYWORDS: Data assimilation Stratosphere Trace species Ultraviolet radiation

1. INTRODUCTION

Over the northern polar cap, column ozone reaches its yearly climatological minimum in late summer or early autumn. The summertime ozone loss is induced by gas-phase chemistry dominated by nitrogen and hydrogen catalytic cycles. These cycles are efficient at high latitudes due to the long summer insolation (see Fahey and Ravishankara 1999). The prominent role of these two cycles in the stratospheric summer chemistry has to be contrasted with the prime importance of the halogen ozone-destroying cycle in winter or spring, when it is activated through heterogeneous chemical processes on the surface of polar stratospheric clouds. Both the Brewer–Dobson mean meridional circulation, which replenishes the Arctic lower stratosphere with ozone-rich air from above, and the planetary-scale waves, which are responsible for its driving and the stirring of midlatitude and polar air, are weaker in summer than in winter. Hence, in the summer Arctic stratosphere, active photochemistry and quieter dynamical conditions allow the formation of a low-ozone pool of air.

At the intraseasonal time-scale, atmospheric motions contribute to the variability of column ozone through vertical and horizontal transport. Column ozone commonly fluctuates over time-scales characteristic of synoptic weather systems, i.e. 2–7 days. These fluctuations peak in the storm-track regions over oceanic areas of the midlatitudes in winter (Orsolini *et al.* 1998). The summer period appears more quiescent with respect to ozone variability on the synoptic time-scale, especially at high latitudes, due to weakened storm tracks. Understanding the nature of the ozone variability from daily to monthly time-scales in the summer polar regions has been hampered by the

* Corresponding author: Norwegian Institute for Air Research, PO Box 100, Instituttveien 18, N-2027 Kjeller, Norway. e-mail: orsolini@nilu.no

scarcity of height-resolved global satellite observations. Previous satellite observations were in solar occultation mode, i.e. limited to narrow latitude bands (Park and Russell 1994; Luo *et al.* 1997; Hoppel *et al.* 1999) or limited in time (Froidevaux *et al.* 1994). Nevertheless, the analysis of mid-stratospheric high-latitude summertime ozone observations by the Polar Ozone and Aerosol Measurement instrument (Hoppel *et al.* 1999) reported planetary-scale westward-propagating patterns that were long-lasting and recurrent. A recent analysis of ozone profiles from the Stratospheric Aerosol and Gas Experiment (Kar *et al.* 2002) showed occurrences of thick ozone-poor layers in the summer high latitudes in the middle stratosphere.

To examine the summertime synoptic evolution of polar ozone, we have assimilated into a chemical trajectory transport model profiles retrieved from the Global Ozone Monitoring Experiment (GOME) satellite instrument (Burrows *et al.* 1999; van der A *et al.* 2002; El Sarafy *et al.* 2002; Eskes *et al.* 2003), and also gathered ozone profiles obtained from electrochemical sondes or lidar at several stations in the European Arctic. While lidars are routinely used to monitor the ozone layer under dark sky conditions (Bird *et al.* 1997; Hansen *et al.* 1997; Orsolini *et al.* 1997), such daylight observations in the summer Arctic have not been attempted before.

The unique combination in summer 2000 of assimilated three-dimensional ozone fields and local observations allowed us to shed some light on ozone variability in the summer polar stratosphere. Figure 1 illustrates that, superimposed upon the near-steady decrease of average column ozone over the Arctic polar cap in late spring and summer 2000, one finds local large-amplitude ozone fluctuations at the high-latitude station of Andøya, northern Norway (69°N, 16°E). The figure shows local Brewer observations, satellite data from the Total Ozone Mapping Spectrometer (TOMS), and assimilated satellite data from the GOME instrument. The week-to-week variations are seen in both satellite datasets despite a slight bias. In July 2000, the TOMS data show a positive bias of about 15 Dobson units (DU) in the polar cap compared with assimilated GOME column ozone. Previous studies of summertime column ozone records at high northern latitudes revealed large distinctive fluctuations with time-scales of several weeks (Lloyd *et al.* 1999), but their origin remained unexplained. We refer to the two pronounced minima observed around early and late July (arrows on Fig. 1) as low-ozone episodes (LOEs), without defining a precise threshold that could only be justified in a climatological study. These minima persist for a few days.

In section 2, we explore further the evolution of column and mid-stratospheric ozone in the Arctic in summer 2000. Further diagnosis based on trajectory calculations combined with ground-based and balloon-borne observations are described in section 3. The impact of these LOEs on ultraviolet (UV) radiation is discussed in section 4. An appendix describes data and modelling tools used in this study.

2. Low-ozone episodes in the Arctic summer

Figure 1 shows the occurrence of several LOEs in July 2000, observed at Andøya. We now demonstrate that the pool of low-ozone air over the Arctic was dynamically disturbed in summer 2000, as implied by the occurrence of intense LOEs. Details of the data-assimilation approach and the lidar instruments are given in an appendix. A sequence of assimilated ozone maps on four different days between 20 June and 26 July 2000, at a pressure level of 30 hPa or about 650 K, reveals a low-ozone pool of air over high latitudes (Fig. 2) that is not zonally symmetric but distorted. This pool undergoes a series of pronounced meridional excursions southwards to 60°N, and covers successively regions of the northern midlatitudes, from Asia to Europe and to North

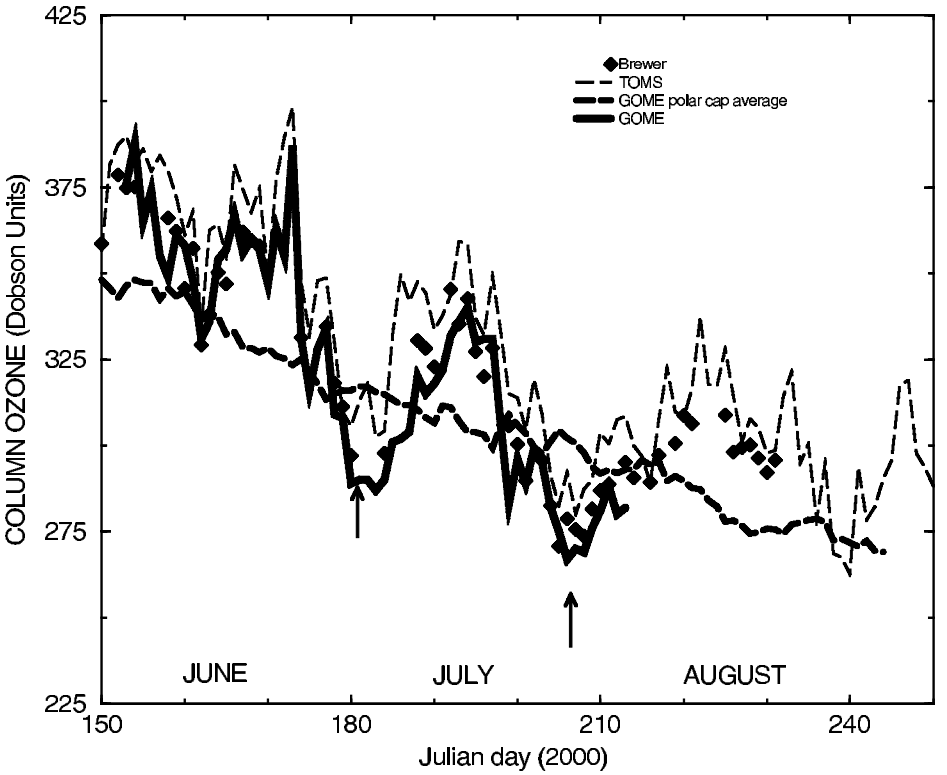

Figure 1. Column ozone derived from transport-model assimilation of Global Ozone Monitoring Experiment (GOME) data in June–July–August 2000. The dashed line shows averaged values over the polar cap (north of 60°N) and the bold line corresponds to Andøya. Brewer and Total Ozone Mapping Spectrometer (TOMS) satellite observations at Andøya are also shown. The two prominent low-ozone episodes in early and late July 2000 are marked with arrows. The GOME data are plotted daily at 0900 UTC. Time is indicated in Julian days. 1 June corresponds to day 153 and 1 July to day 183.

America (e.g. Scandinavia on 6 and 26 July). Inspection of Fig. 2 shows that, following the dominant winds, the low-ozone pool rotates westwards with a period of several weeks. The ensuing large ozone variability at high latitudes is well captured in profiles derived from balloon or lidar. Figure 3, based on a series of weekly *in situ* balloon ozone measurements at Ny-Alesund, Spitsbergen (79°N, 12°E), shows dramatic changes over a broad layer above 50 hPa during July 2000. These variations exceed the standard deviation of ozone fluctuations in July. In the layer 600–850 K, this is about 0.5 ppmv, based on ozone sonde measurements at Ny-Alesund over the years 1992–2002.

At 650 K, the ozone time evolution through June and July 2000, as measured at several Arctic stations by means of sondes or lidar (Fig. 4), is suggestive of two events with large (nearly 50% amplitude) fluctuations in ozone. Both the assimilated ozone maps and the local observations (although the latter are at irregular intervals) are hence indicative of slow planetary-scale motions in the summer stratosphere above 50 hPa.

Planetary-scale waves originating in the troposphere are vertically trapped by westward flow (see Andrews *et al.* 1987). The level of wind reversal, where zonal-mean winds change from eastward to westward, occurs near 20 km in July. Hence some amount of stirring and penetration to the 30 hPa level is expected and has been studied in stratospheric meteorological analyses (Luo *et al.* 1997; Wagner and Bowman 2000).

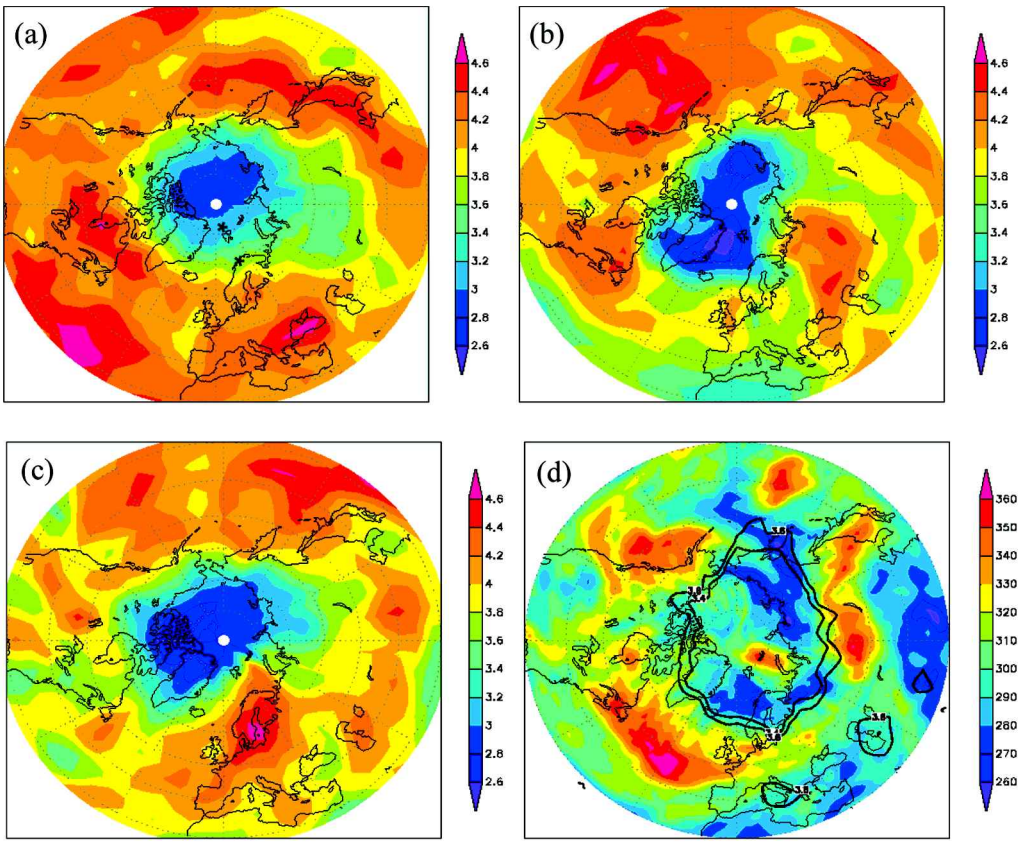

Figure 2. A sequence of ozone maps (ppmv) at pressure level 30 hPa derived from the Global Ozone Monitoring Experiment assimilated dataset for June and July 2000: (a) 20 June, (b) 6 July, (c) 11 July and (d) 26 July. In (d), 3.4 and 3.6 ppmv contours are shown superimposed upon the column ozone map (drawn in Dobson units). The locations of Andøya and Ny-Alesund are marked by stars on (a).

3. Dynamical origin of the low-ozone episodes

In the summer polar stratosphere, the evolution of ozone is governed by coupled dynamical and chemical processes. The week-to-week ozone variations observed by the sondes and lidars (Figs. 3 and 4) are largely caused by meridional motions, as can be understood from the results of chemical-trajectory calculations. Using a stratospheric chemical-box model, we calculated the abundance of 64 key species along a series of backward 10-day trajectories ending at the stations every day from late June to late July 2000. The trajectories are calculated on isentropic surfaces following the adiabatic motion of air parcels. The initial distributions of chemical species were derived from a two-dimensional latitude–height model climatology. The stratospheric chemical-box model allows an extensive diagnosis of atmospheric chemistry, but only ozone is discussed in this paper. Further details of the trajectory model are given in the appendix.

The daily reconstructed ozone at 650 K (Fig. 4, full line) matches remarkably the lidar and sonde observations, including the two troughs and crests separated by 3–4 weeks in July. The succession of ozone crests and troughs is also reproduced in a passive ozone tracer (Fig. 4, dashed line), obtained by turning off chemical tendencies along the trajectories. Hence, while significant ozone destruction is occurring along

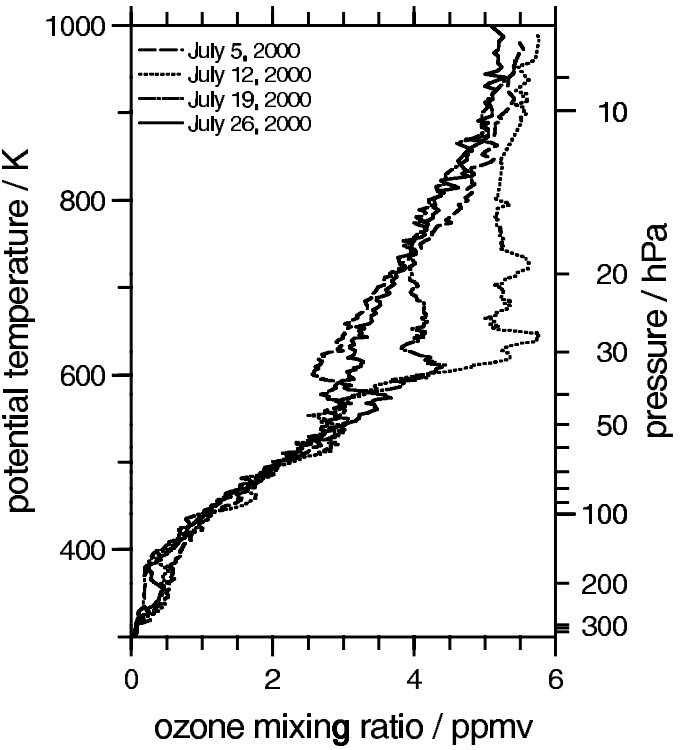

Figure 3. Ozone mixing-ratio profiles as measured on a weekly basis by *in situ* balloon sondes in July 2000 at Ny-Alesund. The vertical coordinate is potential temperature, with approximate pressure levels indicated on the right-hand vertical axis.

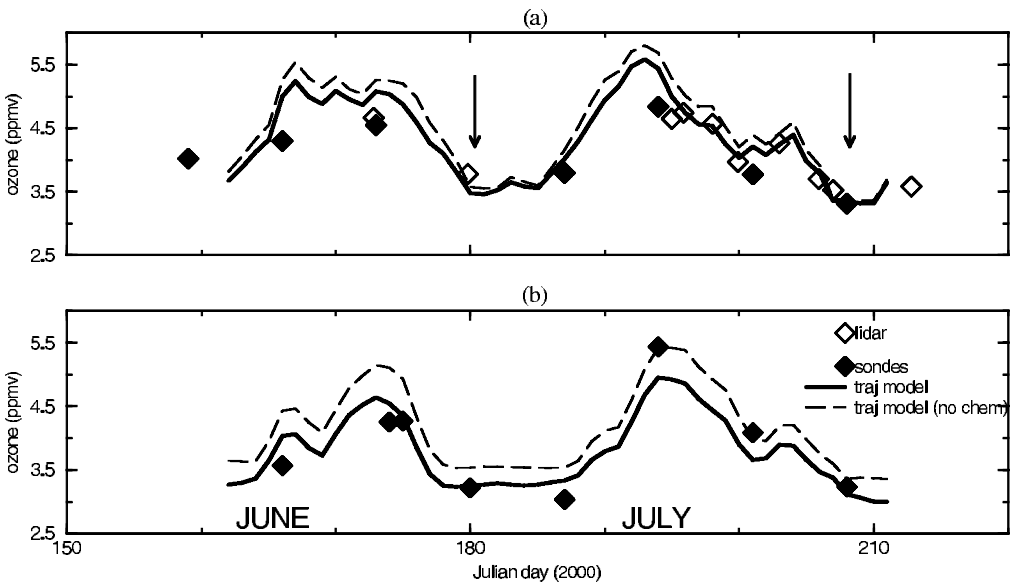

Figure 4. (a) Ozone evolution at the 650 K level through June and July 2000 derived from daylight differential absorption lidar observations (hollow diamonds; at Andøya) and sondes (filled diamonds; at Sodankyla, 450 km east of Andøya). (b) Same for Ny-Alesund, where only sondes are available. The reconstructed ozone (full line) and passive ozone (dashed line) from the trajectory model are also shown.

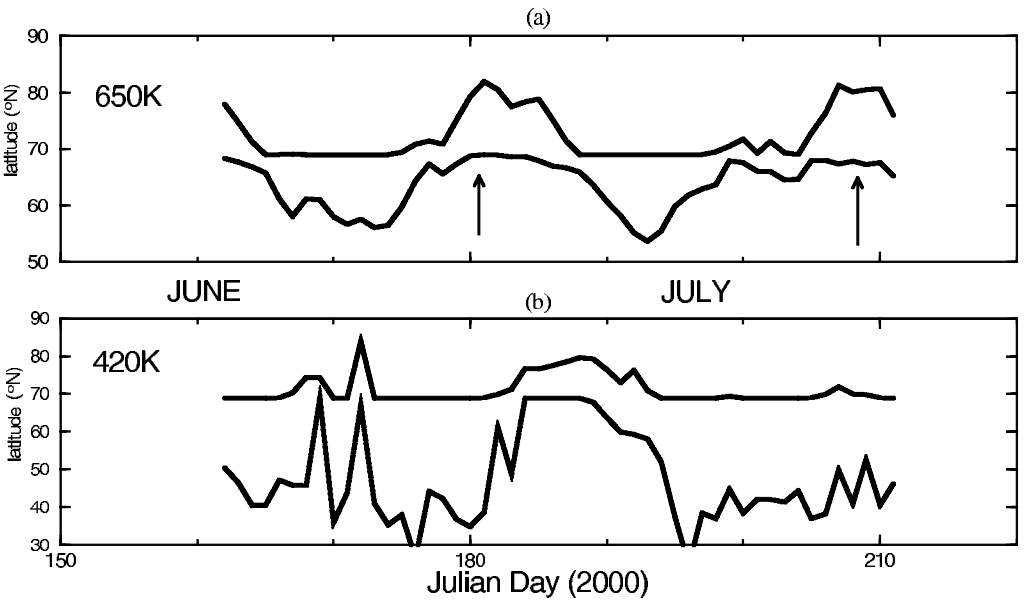

Figure 5. (a) Latitude range along the 10-day trajectories ending at Andøya for each day from mid-June to end of July 2000 at the level of 650 K. During the two low-ozone episodes in early and late July, parcels were mostly north of Andøya during the 10-day time span of the trajectory. (b) As (a) but for 420 K.

these trajectories, amounting up to 30 ppbv day^{-1}, Fig. 4 clearly indicates that the phenomenon of LOEs is largely dynamically induced. However, it is worth noting that the background low ozone in the polar region is driven by photochemistry.

We calculated the latitude bounds for each of the 50 back-trajectories ending at Andøya over the June–July period. These bounds bracket the range of latitudes that air parcels visited in the 10 days before arriving above Andøya, and are shown on Fig. 5. Joint examination of Figs. 4 and 5 indicates that low ozone occurred at 650 K when air parcels originated from the north, while air parcels coming from the south brought in ozone-rich air. This concurs with the GOME assimilation results, linking low-ozone values to meridional displacements of the Arctic low-ozone pool.

Further analysis of the Andøya back-trajectories at lower levels (Fig. 5(b)) indicated that, especially during the late July LOE, while the Arctic low-ozone pool was aloft, air masses originated from the south at low levels. Because the meridional ozone gradient reverses with altitude, these air masses brought ozone-poor air to Andøya, as did the upper-level (e.g. 650 K) air masses. Using the GOME assimilated data, we calculated the contributions to the column ozone at Andøya in two broad layers, in the lower stratosphere (110 to 60 hPa) and in the mid stratosphere (60 to 20 hPa), and found them to be nearly equal on 26 July.

Figure 6 shows the geopotential height at 100 hPa on 26 July subtracted from the July mean. The negative anomalies centred between Scandinavia and Greenland, and over west Eurasia and the North Pacific, correspond to elevated geopotential heights, anticyclonic flow and low column ozone. Positive anomalies, corresponding to lowered geopotential heights, are seen over the Arctic Ocean and the Alaskan coasts. The low-ozone pool aloft contributed to either intensifying or cancelling these low stratospheric ozone anomalies, and is seen to influence the ozone column over a large region of the northern latitudes. Indeed, Fig. 2 shows the wide region of the Arctic and northern

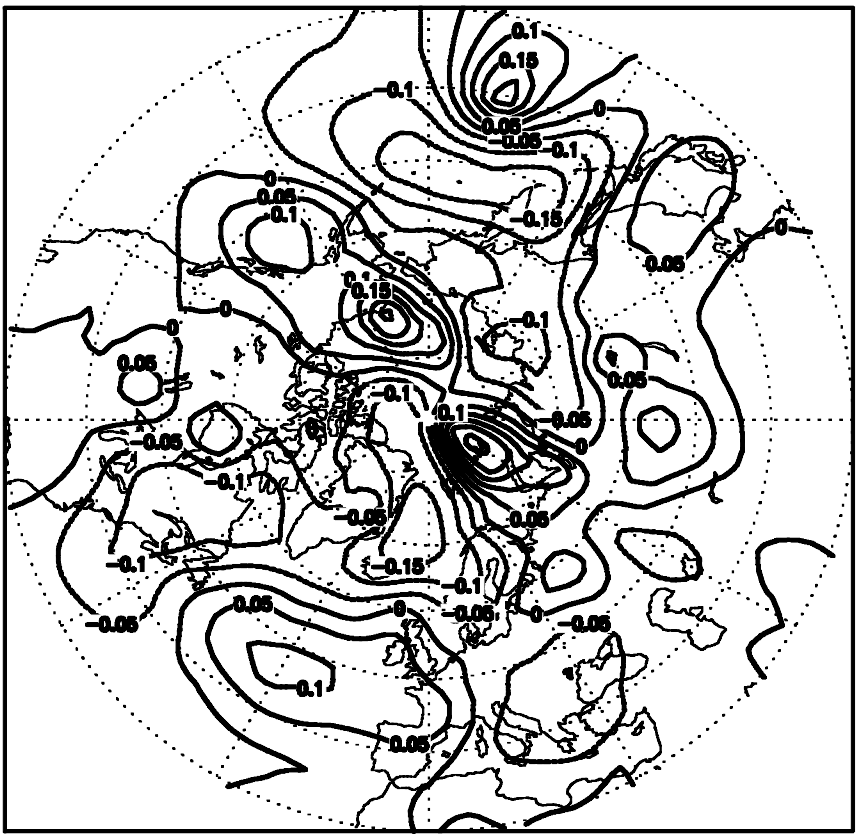

Figure 6. Geopotential height anomaly (km) at 100 hPa on 26 July 2000, obtained by subtracting the height for that day from the July mean. Operational analyses from the ECMWF were used.

midlatitudes with lowered ozone column bordered by the low-ozone mid-stratospheric pool (e.g. contours of 3.4–3.6 ppmv).

Hence intense LOEs are generated by the conjunction of events at different levels, and bear some similarity to winter LOEs (also called miniholes). While the summer episodes have not been mentioned as such in the literature, the former are well studied (Newman *et al.* 1988; McKenna *et al.* 1989; Orsolini *et al.* 1995; Orsolini and Limpasuvan 2001; Hood *et al.* 2001; Bojkov and Balis 2001). They have been shown to result from ozone-poor poleward and upward advection in the lower stratosphere, further reinforced when the ozone-poor winter polar vortex is aloft (James *et al.* 2000; Allen and Nakamura 2002). While wintertime miniholes are commonly linked to travelling synoptic eddies, further analysis of summer episodes is needed to establish whether they are associated with transient or longer-lasting blocking events in the troposphere.

4. Impact on ultraviolet radiation reaching the ground

The thinner the ozone layer, the more UV radiation reaches the ground, where it can impact on human health and ecosystems. The impact of LOEs on surface UV radiation over northern Europe is likely to be large in the summer due to the relatively high solar elevation and long hours of sunlight. Kylling *et al.* (2000) observed large fluctuations in the daily erythemal dose in summer 1997 at Tromsø, Norway

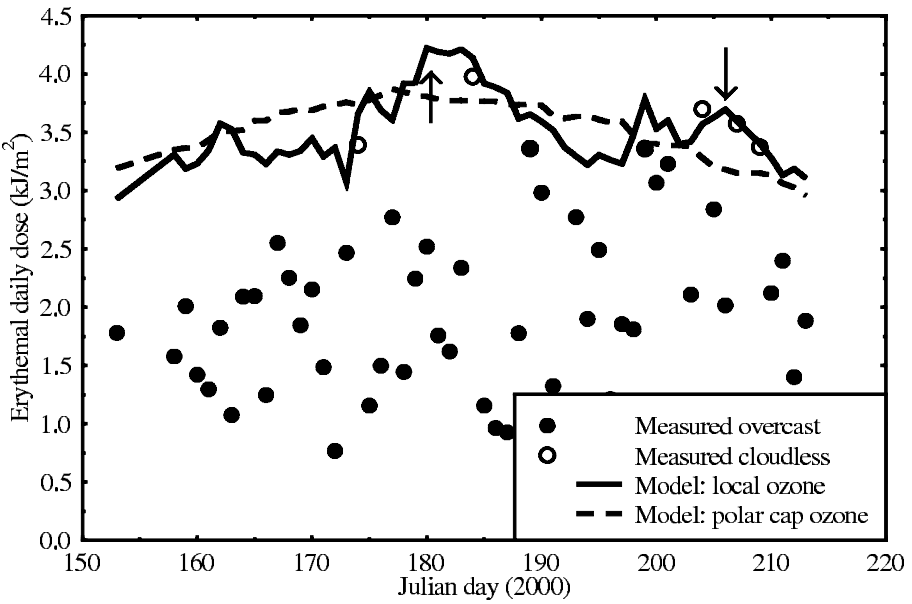

Figure 7. Daily erythemal dose measured at Andøya through June–July 2000, with cloudless model calculations using polar cap average and local column ozone from GOME, as in Fig. 1.

(69°N, 19°E), associated with large-amplitude ozone variations. (The daily erythemal dose is the UV radiation weighted with the Commission Internationale de l'Eclairage action spectrum and integrated over the day.)

We used both the local column ozone over Andøya and the polar cap average (Fig. 1) as input to a well-tested and verified radiative-transfer model (Mayer *et al.* 1997; Kylling *et al.* 1998). In Fig. 7, the resulting simulated daily erythemal dose is shown through June and July 2000 together with the measured daily UV erythemal doses. Measurements are taken from a UV radiometer (GUV-541) from Biospherical Instruments Inc., a multichannel moderate-bandwidth instrument which provides high time-resolution measurements of the erythemal dose rate and effective cloud optical depth. Most of the time the measurements are well below the cloudless-model calculations, indicating cloudiness. For the days clearly identified as cloudless, the model simulations and the measurements are in agreement. During the LOEs in early and late July, the cloudless-model simulations based on local ozone are 10–16% higher than those based on polar cap ozone. Despite the smaller ozone amount during the late July LOE, the UV enhancement is higher during the early July LOE when the solar zenith angle was smaller by about 4°. Thus, LOEs increase the UV radiation above background conditions by a significant amount. A cloud-free atmosphere in prevailing high-tropopause conditions and low column ozone are conducive to this enhancement.

5. Conclusions

While the existence of a low-ozone pool of stratospheric air, akin to an ozone hole, in the summer Arctic is known, its impact on column ozone variability at mid and high latitudes has not been fully realized. We describe how it is implied in hitherto poorly documented phenomena, which consist of episodic lowerings of the column ozone at northern latitudes in summer. Using ground-based balloon-borne observations and

satellite-data assimilation, we have demonstrated that particularly intense episodes over northern Norway in July 2000 occurred in connection with a meridional excursion of the mid-stratospheric pool of low-ozone air that resides over the Arctic. These LOEs are dynamically induced although the background low ozone over the Arctic is caused by an active photochemistry. Interannual variability of these phenomena needs to be studied further.

A strong prolonged winter–spring ozone depletion, like the one observed in 1999–2000, leads to low ozone columns as starting conditions for the summer period. In this way the heterogeneous ozone chemistry during winter–spring could favour more pronounced LOEs.

Enhanced levels of UV radiation during summer at high northern latitudes are observed in connection with the LOEs. Albeit of a temporary nature, the UV enhancement is of the order of the spring increase in UV dose at northern mid or high latitudes caused by halogen-induced ozone depletion (Slaper *et al.* 1996).

The northern hemisphere lower and middle stratosphere in summer appears more dynamically active than previously thought, at least in the year 2000. The ozone variability is linked to planetary-wave motions that have been little studied. Occurrence of summertime LOEs and their connection to tropospheric synoptic conditions need to be examined further. While the coupling of the tropospheric and stratospheric circulations in summer is weaker than in winter, when it is both strong and deep, it nevertheless deserves more attention, in the light of its importance for understanding ozone seasonal variability and trends.

Acknowledgements

This study was supported by the Commission of the European Communities Environment and Sustainable Development programme under project EVK2-CT-1999-000049. The lead author thanks Prof. Høv for reading the first draft.

Appendix

Data and models used in this study are now briefly described. The GOME instrument (Burrows *et al.* 1999) is a high-resolution UV-visible spectrometer, which allows ozone profile information to be retrieved. Ozone profiles were retrieved (van der A *et al.* 2002) for all GOME observations in the period from March to July 2000. These were subsequently assimilated in the TM3 transport model driven by European Centre for Medium-Range Weather Forecasts (ECMWF) meteorological data, based on a simplified Kalman-filter assimilation technique (El Sarafy *et al.* 2002). The ozone assimilation was carried out at a resolution of 3.75° by 5° of latitude and longitude and 23 vertical pressure levels spanning the tropopause and the stratosphere, including nine levels in the stratosphere.

The 10-day backward isentropic trajectories were calculated with the Norsk Institut for Luftforsking Lagrangian box model (De Haan *et al.* 1997). The winds were derived from the ECMWF 60-level analyses, extending from ground to about 60 km altitude. The current model includes the newest kinetic data and recent updates on nitrogen chemistry.

The Norwegian ozone lidar system at the Arctic Lidar Observatory for Middle Atmosphere Research is a standard ozone differential absorption lidar, providing vertical ozone density profiles in the stratosphere (10 to 45 km altitude), with an effective resolution of typically 500 m at heights below 25 km, gradually decreasing with increasing

altitude. The typical time resolution is one hour. These characteristics are valid for the standard operation mode under darkness conditions, which do not apply when the sun is above or only slightly below the horizon at Andøya. To perform the measurements in summer 2000, a dedicated daylight receiver was installed, aiming at operational capability irrespective of illumination conditions. This was achieved by inserting extremely narrow-band spectral filters. The filters consisted of an interference filter combined with a moderately narrow-band Fabry–Perot etalon in the ozone extinction channel (308 nm) and a combination of an interference filter and a very narrow-band double Fabry–Perot etalon system in the reference channel (353 nm). To our knowledge, such a UV receiver filtering system has not been installed at any other ozone lidar system so far. In summer 2000, the signal-to-noise ratio in the 353 nm channel was not sufficient to yield ozone profiles of satisfactory quality. Therefore, this signal (which only reflects Rayleigh scattering from air) was replaced by a profile calculated from radiosondes launched at Andøya (four occasions) or ECMWF data at the closest grid point and time. This method has proved to be very robust except near the tropopause.

References

Allen, D. R. and Nakamura, N. 2002 Dynamical reconstruction of the record low column ozone over Europe on 30 November 1999. *Geophys. Res. Lett.*, **29,** 1362, doi:10.1029/2002GL014935

Andrews, D. G., Holton, J. R. and Leovy, C. B. 1987 *Middle atmosphere dynamics.* Academic Press, New York

Bird, J. C., Pal, S. R., Carswell, A. I., Donovan, D. P., Manney, G. L., Harris, J. M. and Uchino, O. 1997 Observations of ozone structures in the polar vortex. *J. Geophys. Res.*, **102,** 10785–10800

Bojkov, R. D. and Balis, D. S. 2001 Characteristics of episodes with extremely low ozone values in the northern middle latitudes 1957–2000. *Ann. Geophys.*, **19,** 797–807

Burrows, J. P., Weber, M., Buchwitz, M., Rozanov, V., Ladstatter-Weissenmayer, A., Richter, A., De Beek, R., Hoogen, R., Bramstedt, K., Eichmann, K.-U. and Eisinger, M. 1999 The Global Ozone Monitoring Experiment: Mission concept and first scientific results. *J. Atmos. Sci.*, **56,** 151–175

De Haan, D. O., Fløisand, I. and Stordal, F. 1997 Modelling studies of the effects of the heterogeneous reaction ClOOCl+HCl to Cl2+HOOCL on stratospheric chlorine activation and ozone depletion. *J. Geophys. Res.*, **102,** 1251–1258

El Sarafy, G. Y., van der A, R. J., Eskes, H. J. and Kelder, H. M. 2002 Assimilation of a 3D ozone field in global chemistry transport models using a Kalman filter. *Adv. Space. Res.*, **30,** 2473–2478

Eskes, H. J., van Velthover, P., Valks, P. and Kelder, H. M. 2003 Assimilation of GOME total-ozone satellite observations in a three-dimensional tracer-transport model. *Q. J. R. Meteorol. Soc.*, **129,** 1663–1681

Fahey, D. W. and Ravishankara, A. R. 1999 Summer in the stratosphere. *Science*, **285,** 208–210

Froidevaux, L., Waters, J. W., Read, W. G., Elson, L. S., Flower, D. A. and Jarnot, R. F. 1994 Global ozone observations from the UARS MLS: An overview of zonal-mean results. *J. Atmos. Sci.*, **51,** 2846–2866

Hansen, G., Svenøe, T., Chipperfield, M. P., Dahlback, A. and Hoppe, U. P. 1997 Evidence of substantial ozone depletion in winter 1995/96 over northern Norway. *Geophys. Res. Lett.*, **24,** 799–802

Hood, L. L., Soukharev, B. E., Fromm, M. and McCormack, J. P. 2001 Origin of extreme ozone minima at middle to high northern latitudes. *J. Geophys. Res.*, **106,** 20925–20940

Hoppel, K. W., Bowman, K. P. and Bevilacqua, R. M. 1999 Northern hemisphere summer ozone variability observed by POAM II. *Geophys. Res. Lett.*, **26,** 827–830

James, P. M., Peters, D. and Waugh, D. W. 2000 Very low ozone episodes due to polar vortex displacement. *Tellus*, **52B,** 1123–1137

Kar, J., Trepte, C. R., Thomason, L. W. and Zawodny, J. M. 2002 Observations of layers in ozone vertical profiles from SAGE-II (v 6.0) measurements. *Geophys. Res. Lett.*, **29,** 10, doi:10.1029/2001GL014230

Kylling, A., Bais, A. F., Blumthaler, M., Schreder, J., Zerofos, C. S. and Kosmidis, E. 1998 The effect of aerosols on solar UV irradiances during the Photochemical Activity and Solar Ultraviolet Radiation campaign. *J. Geophys. Res.*, **103,** 26051–26060

Kylling, A., Dahlback, A. and Mayer, B. 2000 The effects of clouds and surface albedo on UV irradiances at a high latitude site. *Geophys. Res. Lett.*, **27,** 1411–1414

Lloyd, S., Swartz, W. H., Kusterer, T., Anderson, D., McElroy, C. T., Midwinter, C., Hall, R., Nassim, K., Jaffe, D., Simpson, W., Kelley, J., Nicks, D., Griffin, D., Johnson, B., Evans, R., Quincy, D., Oltmans, S., Newman, P., McPeters, R., Labow, G., Moy, L., Seftor, C., Toon, G., Sen, B. and Blavier, J.-F. 1999 Intercomparison of total ozone observations at Fairbanks, Alaska, during POLARIS. *J. Geophys. Res.*, **104,** 26767–26778

Luo, M., Park, J. H., Lee, K. M., Russell III, J. M. and Bruehl, C. 1997 An analysis of HALOE observations in summer high latitudes using airmass trajectory and photochemical model calculations. *J. Geophys. Res.*, **102,** 16145–16156

McKenna, D., Jones, R. L., Austin, J., Browell, E. V., McCormick, M. P., Kreuger, A. J. and Tuck, A. F. 1989 Diagnostics studies of the Antarctic vortex during the 1997 airborne Antarctic ozone experiment: ozone miniholes. *J. Geophys. Res.*, **94,** 11641–11668

Mayer, B., Seckmeyer, G. and Kylling, A. 1997 Systematic long-term comparison of spectral UV measurements and UVSPEC modeling results. *J. Geophys. Res.*, **102,** 8755–8767

Newman, P. A., Lait, L. R. and Schoeberl, M. R. 1988 The morphology and meteorology of southern hemisphere spring total ozone miniholes. *Geophys. Res. Lett.*, **15,** 923–926

Orsolini, Y. J. and Limpasuvan, V. 2001 The NAO and the occurrences of ozone miniholes. *Geophys. Res. Lett.*, **28,** 4099–4102

Orsolini, Y. J., Cariolle, D. and Deque, M. 1995 Ridge formation in the lower stratosphere and its influence on ozone transport: a GCM study during late January 1992. *J. Geophys. Res.*, **100,** 11113–11135

Orsolini, Y. J., Hansen, G., Hoppe, U. P., Manney, G. L. and Fricke, K. H. 1997 Dynamical modelling of wintertime lidar observations in the Arctic: Ozone laminae and ozone depletion. *Q. J. R. Meteorol. Soc.*, **123,** 785–800

Orsolini, Y. J., Stephenson, D. B. and Doblas-Reyes, F. J. 1998 Storm track signature in total ozone during northern hemisphere winter. *Geophys. Res. Lett.*, **25,** 2413–2416

Park, J. H. and Russell III, J. M. 1994 Summer polar chemistry observations in the stratosphere made by HALOE. *J. Atmos. Sci.*, **51,** 2903–2913

Slaper, H. G., Velders, G. J. M., Daniel, J. S., de Gruijl, F. R. and van der Leun, J. C. 1996 Estimates of ozone depletion and skin cancer incidence to examine the Vienna convention achievements. *Nature.*, **384,** 256–258

van der A, R. J., Van Oss, R. F., Piters, A. J. M., Fortuin, J. P. F., Meijer, Y. J. and Kelder, H. M. 2002 Ozone profile retrieval from recalibrated GOME data. *J. Geophys. Res.*, **107,** doi:10.1029/2001JD000696

Wagner R. E. and Bowman, K. P. 2000 Wavebreaking and mixing in the northern hemisphere summer stratosphere. *J. Geophys. Res.*, **105,** 24799–24808